3-(pyridin-2-yl)imidazo[1,5-a]pyridine (pyridylindolizine) as ligands in complexes of transition and main-group metals.

Celedonio M. Álvarez, Lucía Álvarez-Miguel, Raúl García-Rodríguez, Jose M. Martín-Álvarez and Daniel Miguel *[a]

Abstract:

The coordination of the easily prepared 3-(pyridin-2-yl)imidazo[1,5-a]pyridine (pyridyl aza indolizine, Py-indz) ligand to several metal moieties has been studied, and its electronic properties, similar to the classical ligands 2,2'-bipyridine (bipy) and 1,10-phenanthroline (o-phen) are reported. New complexes have been prepared and fully characterized by X-ray crystallography and other typical spectroscopic methods when possible. Paramagnetic complexes $[Ni(S_2X)_2(Py\text{-}indz)]$ X = $P(OEt)_2$ (**1**), COEt (**2**), $[Ni(acac)_2(Py\text{-}indz)]$ (**3**), $[Ni(Py\text{-}indz)_3](PF_6)_2$ (**4**), $[Mn_2Cl_4(Py\text{-}indz)_2]$ (**6**) and $[MnCl_2(Py\text{-}indz)_2]$ (**7**) have the magnetic moment expected for a metallic cation with two or five unpaired electrons. Diamagnetic complexes show NMR spectra with a similar pattern with small differences depending on the complex**.** $[M(S_2P(OEt)_2)_2$ (Py-indz)] M = Zn (**8**), Cd (**9**) have pentacoordinated and hexacoordinated structures respectively. Octahedral tin complexes $[SnL_4(Py\text{-}indz)]$ $L_4 = I_4$ (**10**), Cl_3Ph (**11**), $Cl_2{}^nBu_2$ (**12**) have different behaviors in solution, while complex **10** is practically insoluble, complex **11** displays the expected pattern in its NMR spectrum, and complex **12** shows dynamic behavior. The Py-indz ligand is also able to stabilize copper (I) and forms $[Cu(PPh_3)_2(Py\text{-}indz)]BF_4$ (**13**). The synthesis of the carbonyl complexes $[MBr(CO)_3(Py\text{-}indz)]$ M = Mn (**14**), Re (**15**) and $[Mo(CO)_4(Py\text{-}indz)]$ (**16**) has been followed by IR spectroscopy in solution. [RuCl*p*-cym(Py-indz)]PF_6 (**17**) has the familiar half-sandwich ''three-legged piano-stool'' geometry.

Introduction

We have recently reported a facile method for the preparation of Mn(II) complexes with 3-(pyridin-2-yl)imidazo[1,5-a]pyridine (pyridyl aza indolizine, Py-indz) acting as chelate ligands. The heterocyclic ligand containing a 9-aza-indolizine skeleton is produced by condensation of two molecules of pyridine-2-carboxaldehyde and one mol of ammonium cation within the coordination sphere of a Mn(II) bis dithiophosphate complex.[1] The Py-indz ligand can be easily removed from the manganese complex and isolated as a high purity crystalline solid. Previous methods based mainly on the cyclization of N-2-pyridylmethyl amines were modestly efficient,[2] and other new routes were proposed, based on the acid-promoted condensation of dipyridylamines,[3] the oxidative condensation of aldehydes with 2-pyridyl-amines,[4],[5] the aza-Wittig reaction on N-vinyl phosphazenes[6] or the cyclization of 2-enynylpyridines,[7] and coupling reactions to provide imidazo[1,5-a]pyridine N-heterocyclic carbene precursors. [8]

There are only a few examples of the use of 3-(pyridin-2-yl)-imidazo[1,5-a]pyridines as ligands in Cu(II),[9] Ni(II),[10] V(V),[11] Ir(III)[12] and Re(I) complexes,[13] or analogues in Cd(II),[14] to prepare boron complexes[15] or involved in catalytic process of N-heterocyclic synthesis.[16] Some related derivatives of 3-(pyridin-2-yl)-imidazo[1,2-a]pyridine have been used in situ to regulate metal-induced amyloid-β aggregation.[17] These ligands with a 2-azaindolizine skeleton have received some attention recently due to their interesting properties[18] and potential pharmacological applications.[19],[20] This prompted us to screen the potential of the now easily available Py-indz ligand in the preparation of complexes. While research on the mechanism and the optimization of the reaction leading to Py-indz is currently in progress in our laboratory we have found that Py-indz can act as a versatile ligand towards a wide range of either transition or main group metals, coexisting with a wide range of accompanying ligands, either soft such as iodide, phosphine or dithiolate, or hard such as nitrogen or oxygen donors, with classic and organometallic fragments. Herein we report the preparation of a variety of complexes with transition and main group metals together with their characterization by spectroscopic and crystallographic methods.

Results and Discussion

In view of the stability and the facile preparation and purification of the derivatives containing the manganese bis-dithiophosphate moiety, we sought to prepare the analogous complexes with nickel using the readily available Ni(II) bis dithiophosphate. The reaction of $[Ni\{S_2P(OEt)_2\}_2]$ with one mol-equivalent of Py-indz gave compound **1** in good yield. The analogous reaction starting from the xanthate gave **2** and using $[Ni(acac)_2(MeOH)_2]$ gave **3** (Scheme 1). Compounds **1-3** were readily purified by recrystallization and their structures were determined using X-ray crystallography (see Figures 1, 2 and Table 1).

[a] GIR MIOMET-IU CINQUIMA
Química Inorgánica, Facultad de Ciencias, Universidad de Valladolid, E-47011 Spain.
dmsj@qi.uva.es

Supporting information for this article is given via a link at the end of the document.

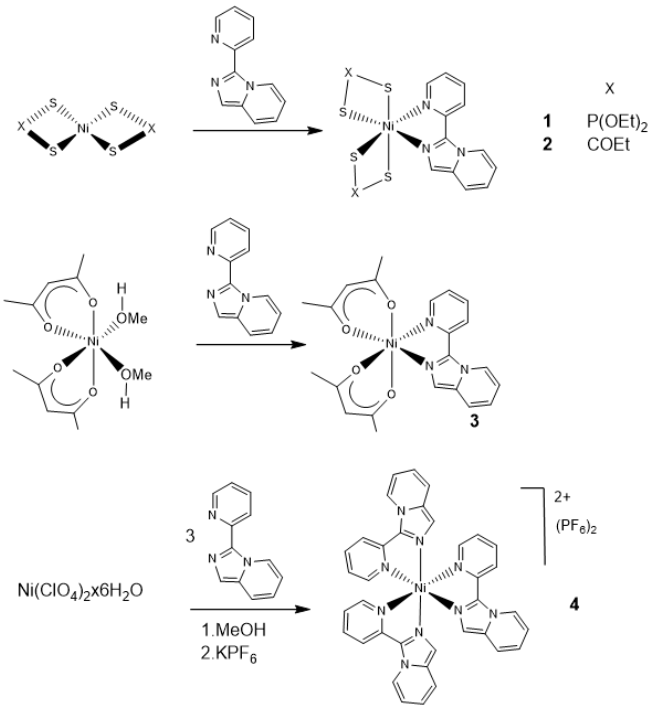

Scheme 1. Synthesis of nickel complexes with Py-indz..

The tris-chelate complex $[Ni(Py\text{-}indz)_3](PF_6)_2$ (**4**), can be obtained by adding three mol-equivalents of Py-indz to nickel perchlorate hexahydrate and subsequent anion exchange with KPF6. The structure of the cation is shown in Figure 3. The values of the magnetic moment at room temperature for Py-indz nickel (II) compounds 1-3 are 2.78, 2.40, 2.78 BM respectively, and 2.90 BM for compound 4 at 20 K. These values indicate the presence of two unpaired electrons, as expected for octahedral Ni(II) complexes.

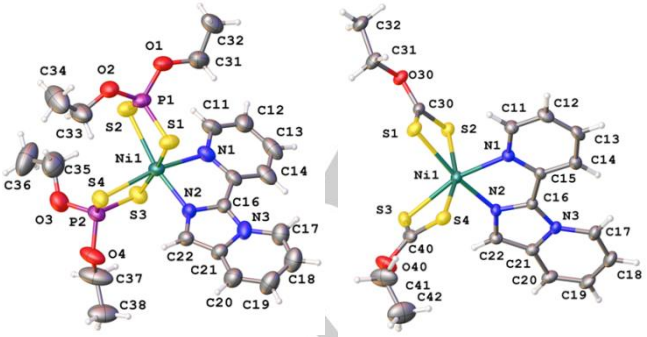

Figure 1. Perspective view of compounds 1 and 2 showing the atom numbering. Selected bond lengths (Å) and angles (º) for 1: Ni(1)-S(1) 2.474(2), Ni(1)-S(2) 2.502(2), Ni(1)-S(3) 2.476(2), Ni(1)-S(4) 2.480(2), Ni(1)-N(1) 2.118(4), Ni(1)-N(2) 2.053(4), S(2)-Ni(1)-S(1) 80.90(5), S(4)-Ni(1)-S(3) 81.78(5), N(2)-Ni(1)-N(1) 78.46 (17). Selected bond lengths (Å) and angles (º) for 2: Ni(1)-S(1) 2.409(1), Ni(1)-S(2) 2.468(1), Ni(1)-S(3) 2.430(1), Ni(1)-S(4) 2.451(1), Ni(1)-N(1) 2.118(2), Ni(1)-N(2) 2.036(2), S(2)-Ni(1)-S(1) 73.06(3), S(4)-Ni(1)-S(3) 73.28(3), N(2)-Ni(1)-N(1) 77.49(9).

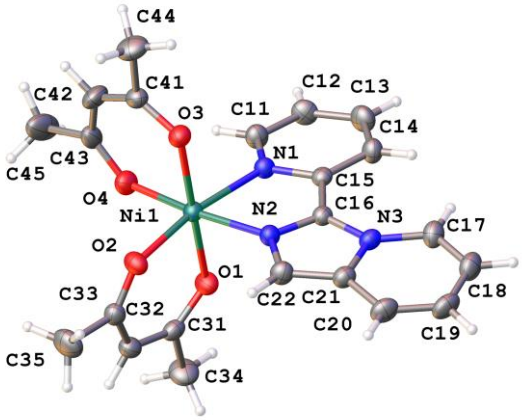

Figure 2. Perspective view of the nickel acetylacetonate derivative 3 showing the atom numbering. Selected bond lengths (Å) and angles (º): Ni(1)-O(1) 2.032(3), Ni(1)-O(2) 2.018(3), Ni(1)-O(3) 2.049(3), Ni(1)-O(4) 2.009(3), Ni(1)-N(1) 2.115(3), Ni(1)-N(2) 2.062(3), O(2)-Ni(1)-O(1) 90.50(12), O(4)-Ni(1)-O(3) 90.49(13), N(2)-Ni(1)-N(1) 77.55(13).

The Py-indz ligand structure is reminiscent to the classical 2, 2'-bipyridine and 1,10-phenanthroline ligands, and we expected the same behavior when coordinated to a transition metal. To test this, tris-Py-indz nickel (II) complexes, analogous to the well known tris-bipy or tris-phen complexes, were prepared using standard methods and their UV-Vis spectroscopic properties measured and summarized in Table 1.

Table 1. UV-Vis spectroscopic properties of tris-nitrogen donor quelate nickel(II) complexes

	Absorption bands (cm^{-1}) and ε ($M^{-1}cm^{-1}$)		Δo	f(10^{-3})	h
$[Ni(phen)_3]^{2+a}$	12700(6,80)	19300(11,90)[a]	12700[a]	1,426[b]	-
$[Ni(bipy)_3]^{2+}$	12650(7,10)[a]	19200(11,60)[a]	12650[a]	1,430[b]	-
	12674(6,33)	19194(12,16)	12674	1,424	2,630
$[Ni(Py\text{-}indz)_3]^{2+}$	12555(6,15)	19011(11,95)	12554	1,410	2,690

[a] Values obtained from C K Jorgensen, *Acta Chem. Scand.* **1955**, *9*, 1362. [b] Values obtained from (1) Figgis, B. N. Introduction to Ligand Field Theory; Interscience: NewYork, **1966**, (2) B.N. Figgis, M.A. Hitchmann, Ligand Field Theory and Its Applications, Wiley, New York, **2000.**

The calculated values of Δo, f and h for tris-Py-indz nickel (II) are similar to the reported values for the bipy and phen Ni(II) complexes confirming that the Py-indz ligand displays electronic effects close to those known for 2,2'-bipyridine and 1,10-phenanthroline.

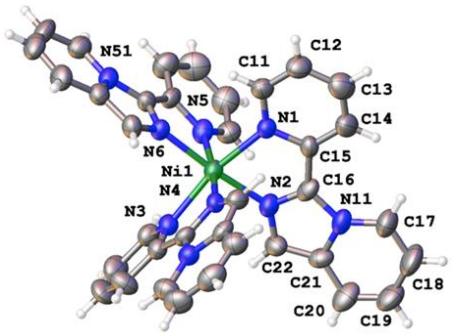

Figure 1. Perspective view of the cation in 4 showing the atom numbering. Selected bond lengths (Å) and angles (º): Ni(1)-N(1) 2.089(5), Ni(1)-N(2) 2.053(6), Ni(1)-N(3) 2.111(5), Ni(1)-N(4) 2.054(5), Ni(1)-N(5) 2.113(6), Ni(1)-N6 2.047(5), N(1)-Ni(1)-N(2) 78.9(2), N(3)-Ni(1)-N(4) 78.4(2), N(5)-Ni(1)-N(6) 77.7(2), N(1)-Ni(1)-N(6) 98.2(2), N(2)-Ni(1)-N(6) 173.6(2).

A similar procedure as for the above nickel complex gave diamagnetic, low spin d^6, $[Fe(Py\text{-}indz)_3](PF_6)_2$ complex (**5**) as a microcrystalline solid. 1D and 2D NMR spectra showed signals of the expected *fac*- and *mer*- isomers, but they were overlapped and it was not possible to make an assignment for each individual isomer (see Experimental Section and Supplementary Information). Despite repeated attempts it was not possible to grow crystals suitable for X-ray analysis for the tris-chelate iron complex **5** but a HRMS (High Resolution Mass Spectrum) could be carried out confirming the empirical formula.

In the case of high-spin d^5 Mn(II) complexes in which there is no Crystal Field Stabilization Energy (CFSE), the structure can be induced by the stoichiometry of the reagents used in the preparation (Scheme 2).

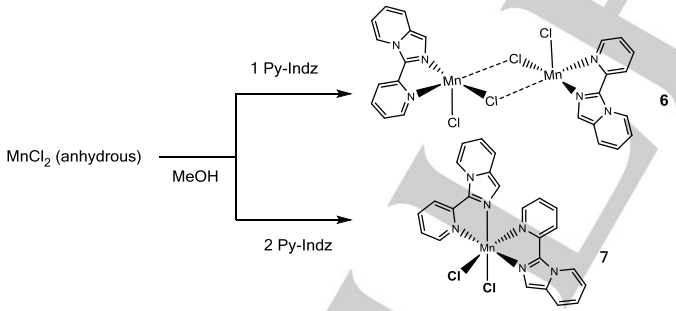

Scheme 1. Synthesis of Mn(II) complexes with Py-indz

Addition of only one mol-equivalent of Py-indz to $MnCl_2$ resulted in the formation of the binuclear complex $[Mn_2Cl_2(\mu\text{-}Cl)_2(Py\text{-}indz)_2]$ (**6**), in which the structure consists of two manganese centers bridged by two chloride atoms. Mn ion lies in a distorted square-pyramidal coordination involving the two N and Cl atoms in the basal plane and one Cl ion in the apical position. Mn atom is displaced 0.720 Å out of the N(1), N(2), Cl(2) and Cl(2A) least squares plane toward the apical halide. This considerable distortion is found in similar binuclear chloride bridged complexes of Mn (II). [21] The addition of two mol-equivalents of Py-indz to $MnCl_2$ produces the expected distorted octahedral $[MnCl_2(Py\text{-}indz)_2]$ (**7**) (Figure 4).

The values of magnetic moments at room temperature for Py-indz adducts of **6** and **7** compounds are 5.65 and 5.84 BM respectively, corresponding to 5 unpaired electrons.

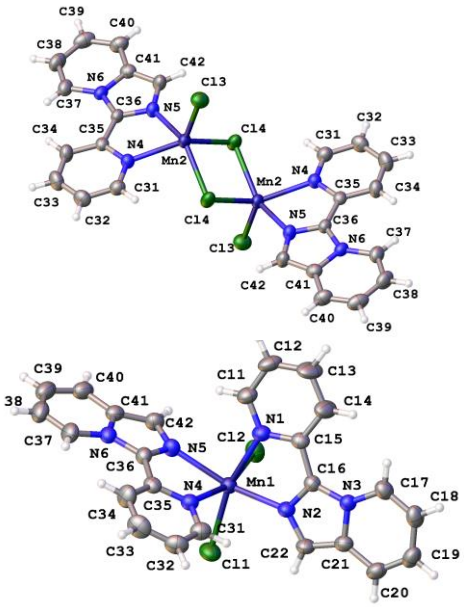

Figure 2. Compounds **6** (left) and **7** (right). Selected bond lengths (Å) and angles (º) of **6**: Mn(1)-N(1) 2.262(2), Mn(1)-N(2) 2.168(2), Mn(1)-Cl(1) 2.336(1), Mn(1)-Cl(2) 2.487(1), Mn(1)-Cl(2A) 2.508(1), N(1)-Mn(1)-N(2) 73.40(8), Cl(1)-Mn(1)-Cl(2) 105.46(3), Cl(1)-Mn(1)-Cl(2A) 108.64(3), Cl(2)-Mn(1)-Cl(2A) 85.89(3). Selected bond lengths (Å) and angles (º) of **7**: Mn(1)-N(1) 2.337(2), Mn(1)-N(2) 2.242(2), Mn(1)-N(3) 2.400(2), Mn(1)-N(4) 2.235(2), Mn(1)-Cl(1) 2.445(1), Mn(1)-Cl(2) 2.442(1), N(1)-Mn(1)-N(2) 70.39(6), N(4)-Mn(1)-N(5) 69.95(6), Cl(1)-Mn(1)-Cl(2) 100.62(2)

The readily available bis dithiophosphates of Zn (II), [22] and Cd (II) can be used as starting materials for the preparation of heteroleptic complexes with N-donor ligands, [23] $[M(S_2P(OEt)_2)_2(Py\text{-}indz)]$, M = Zn (**8**) and Cd (**9**). As can be seen in Figure 5, the cadmium complex **9** is, as expected, hexacoordinate, while the Zn complex **8** is pentacoordinate with the Py-indz and one dithiophosphate ligand acting as bidentate chelate, and the second dithiophosphate acting as monodentate. The Zn(1)-S(4) distance is 4.074(2) Å too long for a significant interaction (*cf* with the bonded Zn(1)-S(3) 2.308(1) Å). This square pyramidal distortion is typical in adducts of bis-dialkyl dithiophosphate Zn (II) complexes. [23 [23b, 23c]

Being diamagnetic, these Zn and Cd complexes could also be characterized by NMR spectroscopy. The $^{31}P\{^1H\}$ NMR spectrum of compound **8** at room temperature display only one signal for the two dithiophosphate ligands, suggesting a fast exchange between the two coordination modes. The dynamic equilibrium is rapid on the NMR time scale and can't be stopped at -50ºC, as deduced from the absence of splitting of the dithiophosphate signals in a low temperature spectrum (-50ºC).

The ^{1}H NMR spectra of compounds **8** and **9** have a representative pattern, similar to the one shown by the Py-indz free ligand, giving signals in the range δ 6.70-10.00 ppm for protons of "pyridine" and "imidazole" rings. Only a few chemical shifts show significant changes when the ligand is coordinated (a Scheme with the correspondence between the signals of the free ligand and the coordinated ligand can be seen in the Supporting Information). The larger shift occurs for the proton attached to C17 (H5) since it is H-bonded to the N1 atom in the free ligand and that H-bond has to be broken upon coordination. A ^{1}H-^{1}H NOESY experiment (supporting information) shows a cross peak between H5 and H3' (proton attached to C14) confirming the assignment of the signals based on $^{13}C\{^{1}H\}$, $^{31}P\{^{1}H\}$, ^{1}H-^{1}H gCOSY, ^{1}H-^{13}C gHSQC, and ^{1}H-^{13}C gHMBC experiments.

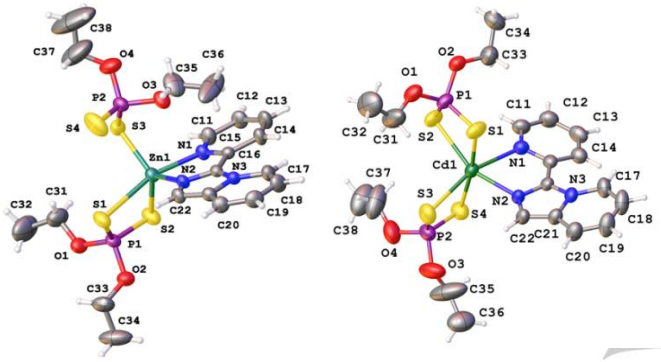

Figure 3. Compounds **8** and **9**. Selected bond lengths (Å) and angles (º) for 8: Zn(1)-S(1) 2.780(1), Zn(1)-S(2) 2.365(1), Zn(1)-S(3) 2.308(1), Zn(1)-S(4) 4.074(2), Zn(1)-N(1) 2.192(2), Zn(1)-N(2) 2.023(2), S(2)-Zn(1)-S(1) 79.26(3), N(2)-Zn(1)-N(1) 77.12(9). Selected bond lengths (Å) and angles (º) for 9: Cd(1)-S(1) 2.734(1), Cd(1)-S(2) 2.649 (1), Cd(1)-S(3) 2.672(1), Cd(1)-S(4) 2.675(2), Cd(1)-N(1) 2.432(3), Cd(1)-N(2) 2.319(3), S(2)-Cd(1)-S(1) 75.77(4), S(3)-Cd(1)-S(4) 76.20(4), N(2)-Cd(1)-N(1) 70.00(10).

A new family of complexes can be obtained by using Lewis acids such as SnI_4, $PhSnCl_3$ or $^{n}Bu_2SnCl_2$ as stating materials. The complexes $[SnI_4(Py\text{-}indz)]$ (**10**), $[SnCl_3Ph(Py\text{-}indz)]$ (**11**), and $[SnCl_2(^{n}Bu)_2(Py\text{-}indz)]$ (**12**), (Scheme 3) were isolated in good yields, and characterized by spectroscopic methods. Their structures are depicted in Figure 6, showing octahedral arrangement around the tin atom. The main distortion from the ideal octahedral geometry comes from the small bite angle, N(1)-Sn(1)-N(2), of the Py-indz ligand (71.6(4), 70.8(2) and 67.53(14) for complexes 10, 11 and 12 respectively).

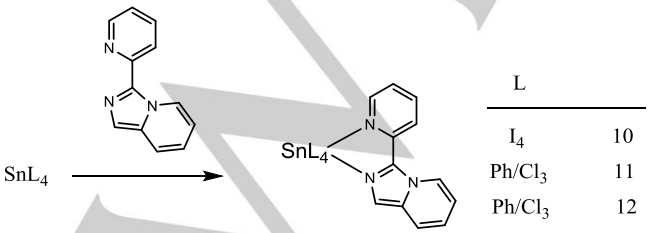

L	
I_4	10
Ph/Cl_3	11
Ph/Cl_3	12

Scheme 3. Synthesis of tin complexes.

It is noticeable that the Sn-halogen (I or Cl) distances are consistently longer when the halogen is in the trans position with respect to other halogen, compared to those in which the halogen is trans to nitrogen. This can be ascribed to the existence of some kind of trans influence, which is greater for the halogen and smaller for the nitrogen ligand. To support this argument, theoretical calculations have been carried out on complex **10**. Starting from the geometry obtained by X-ray diffraction, an optimization at the B3LYP level using the LANL2DZ basis set for Sn and I, and 6-31G(d,p) for the rest of elements, led to a minimum in which the Sn-I distance is longer when another iodine is situated in the trans position. The same effect is seen in the related compound $[SnI_4(bipy)]$ that was reported by Medvedev et al (2.813 and 2.819 Å for the Sn-I distances with another I trans, 2.787 and 2.788 Å for the Sn-I distances with a N atom trans).[24]

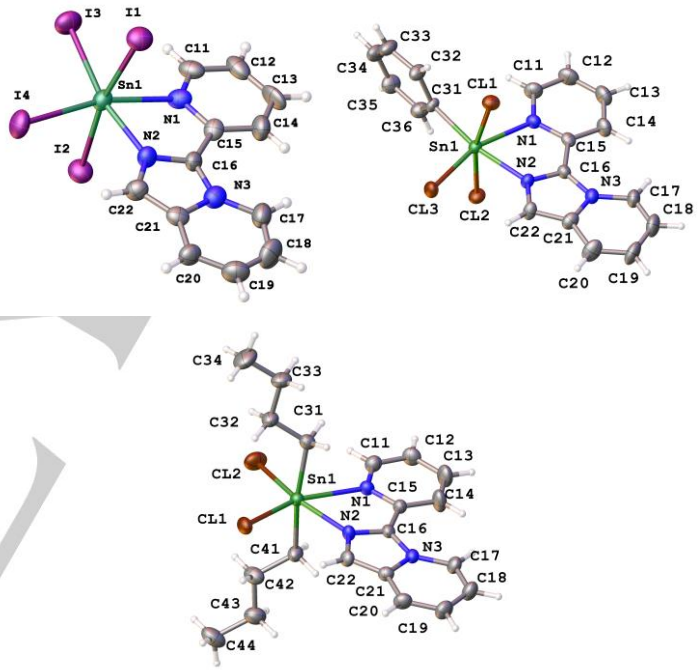

Figure 4. Compounds **10**, **11** and **12**. Selected bond lengths (Å) and angles (º) for **10**: Sn(1)-I(1) 2.821(1), Sn(1)-I(2) 2.829(1), Sn(1)-I(3) 2.741(1), Sn(1)-I(4) 2.767(1), Sn(1)-N(1) 2.303(10), Sn(1)-N(2) 2.212(10), I(2)-Sn(1)-I(1) 169.87(4), I(1)-Sn(1)-I(3) 93.14(4), I(3)-Sn(1)-I(4) 100.65(4), N(2)-Sn(1)-N(1) 71.6(4). Selected bond lengths (Å) and angles (º) for **11**: Sn(1)-Cl(1) 2.454(2), Sn(1)-Cl(2) 2.462(2), Sn(1)-Cl(3) 2.389(2), Sn(1)-C(31) 2.171(7), Sn(1)-N(1) 2.311(6), Sn(1)-N(2) 2.186(6), Cl(2)-Sn(1)-Cl(1) 165.99(7), Cl(2)-Sn(1)-Cl(3) 91.78(8), Cl(3)-Sn(1)-C(31) 101.97(19), N(2)-Sn(1)-N(1) 70.8(2). Selected bond lengths (Å) and angles (º) for **12**: Sn(1)-Cl(1) 2.511(1), Sn(1)-Cl(2) 2.534(2), Sn(1)-C(31) 2.123(5), Sn(1)-C(41) 2.128(5), Sn(1)-N(1) 2.439(4), Sn(1)-N(2) 2.366(4), Cl(2)-Sn(1)-Cl(1) 106.28(5), Cl(1)-Sn(1)-C(31) 94.60(15), C(31)-Sn-C(41) 170.34(19), N(2)-Sn(1)-N(1) 67.53(14)

Tin complexes **10, 11** and **12** are diamagnetic and can be studied by NMR in solution but, unfortunately, compound **10** couldn't be dissolved in the usual deuterated solvents. Complex **11** gives the representative pattern discussed above, but complex **12** shows a more complicated spectrum. At room temperature most of the signals of aromatic protons of **12** are so broad that they are indistinguishable from the baseline, suggesting some kind of dynamic process in solution. At lower temperature the process rate is reduced and at -50ºC the nine signals corresponding to the Py-indz ligand chelated to metal can be observed although they are still very broad (see Figure 7). The low temperature spectrum is consistent with the structure observed in solid state by X-ray diffraction. At 20ºC the spectrum shows the expected well resolved sharped signals corresponding to the butyl ligands but they are

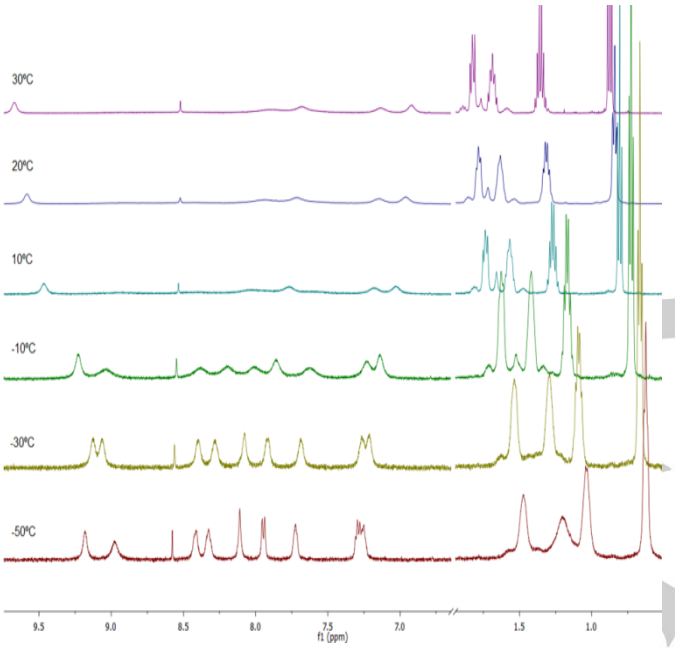

Figure 7. Variable temperature 1H NMR spectra of complex **12**. For clarity, only the aromatic proton range (10.0 to 6.3 ppm), and the alkyl proton range (2.0 to 0.0 ppm) are shown. An impurity appears at 8.58 ppm.

Addition of Py-indz to $[Cu(PPh_3)_2(NCMe)_2]BF_4$ produces the substitution of the acetonitrile ligands to afford $[Cu(PPh_3)_2$(Py-indz)$]BF_4$ (**13**) as a yellow crystalline solid. The structure (Figure 8) shows a tetrahedral disposition around the copper atom. Again the main distortion corresponds to the small bite angle of the Py-indz ligand N(1)-Cu-N(2), with a value of 79.49(9), very similar to the one found in bipy Cu (II) analogous complexes. [25]

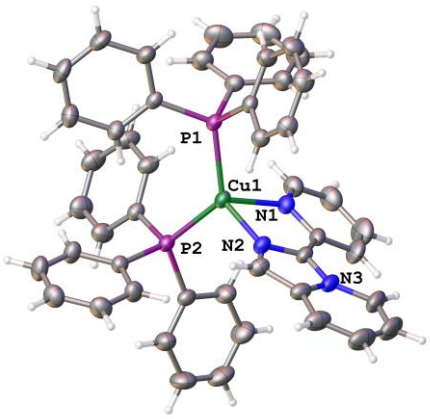

Figure 8. Cation of Compound **13**. Selected bond lengths (Å) and angles (º): Cu(1)-N(1) 2.115(2), Cu(1)-N(2) 2.067(2), Cu(1)-P(1) 2.257(1), Cu(1)-P(2) 2.271(1), N(1)-Cu(1)-N(2) 79.49(9), P(1)-Cu(1)-P(2) 125.07(3), N(1)-Cu(1)-P(1) 107.50(7), N(1)-Cu(1)-P(2) 106.80(7), N(2)-Cu(1)-P(1) 119.30(7)

Diimine ligands such as bipy or phen, have been used extensively as ancillary ligands in carbonyl complexes of middle transition metals. Py-indz can be used in thermally induced substitution reactions in the same way as bipy or phen. Thus, reaction with bromopentacarbonyl complexes of manganese or rhenium, or with molybdenum hexacarbonyl, produced $[M(CO)_3$(Py-indz)Br], M = Mn (**14**), Re (**15**), or $[Mo(CO)_4$(Py-indz)] (**16**) as depicted in Scheme 5. We have been interested in complexes containing pyridine-2-carboxaldehyde (pyca) as chelating κ^2 (N,O) ligands which can serve as precursors for the introduction of metal-ligand fragments in biomolecules.[26]

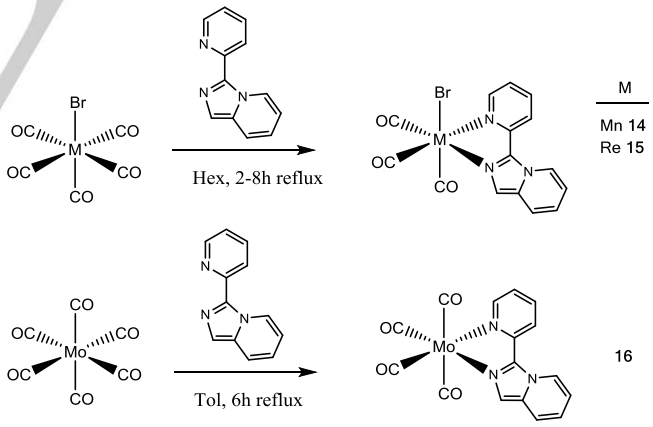

Scheme 2. Synthesis of carbonyl complexes with Py-indz.

The ν(CO) bands of the coordinated carbonyls can be easily observed by IR spectroscopy in solution. The three band pattern expected for a fac-tricarbonyl arrangement appears at frequencies close to those observed for the bipy and phen analogues [27] (see Table 2).

Table 2. Carbonyl stretching frequencies (cm^{-1}, THF solution)[a]

	ν_1(ms)	ν_2(s)	ν_3(s)
$[Mn(CO)_3Br(Py\text{-}indz)]$	2022	1934	1911
$[Mn(CO)_3Br(bipy)]$	2023	1935	1915
$[Mn(CO)_3Br(phen)]$	2024	1936	1915
$[Re(CO)_3Br(Py\text{-}indz)]$	2018	1917	1891
$[Re(CO)_3Br(bipy)]$	2020	1920	1896
$[Re(CO)_3Br(phen)]$	2021	1920	1897

	ν_1(m)	ν_2(s)	ν_3(m, sh)	ν_1(m)
$[Mo(CO)_4(Py\text{-}indz)]$	2010	1895	1878	1838
$[Mo(CO)_4(bipy)]$	2013	1901	1883	1842
$[Mo(CO)_4(phen)]$	2012	1901	1884	1842

[a] For a more accurate comparision, the spectra of the complexes with bipy and phen have been taken in the same solvent and measured with the same instrument.

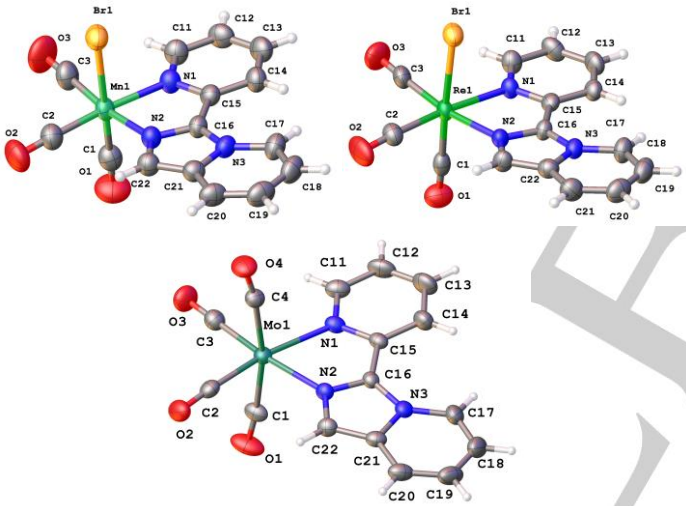

Figure 9. Compounds **14**, **15** and **16**. Selected bond lengths (Å) and angles (º) for **14**: Mn(1)-Br(1) 2.548(1), Mn(1)-N(1) 2.066(2), Mn(1)-N(2) 2.016(2), Mn(1)-C(1) 1.787(4), Mn(1)-C(2) 1.795(3), Mn(1)-C(3) 1.794(4), C(2)-Mn(1)-C(1) 89.15(16), C(2)-Mn(1)-C(3) 88.89(16), C(2)-Mn(1)-Br(1) 91.68(11), N(2)-Mn(1)-N(1) 78.63(9). Selected bond lengths (Å) and angles (º) for **15**: Re(1)-Br(1) 2.636(1), Re(1)-N(1) 2.190(4), Re(1)-N(2) 2.158(4), Re(1)-C(1) 1.904(7), Re(1)-C(2) 1.897(6), Re(1)-C(3) 1.921(7), C(2)-Re(1)-C(1) 88.0(2), C(2)-Re(1)-C(3) 88.5(2), C(2)-Re(1)-Br(1) 94.95(18), N(2)-Re(1)-N(1) 74.59(16). Selected bond lengths (Å) and angles (º) for **16**:, Mo(1)-N(1) 2.271(3), Mo(1)-N(2) 2.200(3), Mo(1)-C(1) 2.010(4), Mo(1)-C(2) 1.944(4), Mo(1)-C(3) 1.952(4), Mo(1)-C(4) 2.027(4) C(2)-Mo(1)-C(1) 84.01(15), C(2)-Mo(1)-C(3) 90.97(16), C(2)-Mo(1)-C(4) 87.67(15), N(2)-Mo(1)-N(1) 71.83(10).

Finally, Ru(II) complex **17** was obtained through the reaction of [RuCl(p-cym)(NCMe)2]PF6 and Py-indz ligand. The complex has the familiar half-sandwich ‘‘three-legged piano-stool’’ geometry with the η6- π-bound arene ring forming the seat, and the two nitrogen atoms of the ligand and one terminal chloride ligand as the legs of the piano-stool. The arene is formally covering three facial coordination sites. If the center of the aromatic ring is considered as a single site, the Ru environment may be regarded as tetrahedral with a significant trigonal distortion. The Ru distance to the centroid (called Cent from now on) of the aromatic ring was found to be 1.676(5) Å. The Cl(1)–Ru(1)–N(1), Cl(1)–Ru(1)–N(2) and N(1)–Ru(1)–N(2) angles are 85.85(11)°, 84.66(12)° and 76.23(15)° respectively, while the angles Cl(1)–Ru(1)–Cent 128.27(2)°, N(1)–Ru1–Cent 131.29(2)° and N(2)–Ru(1)–Cent 132.15(2)° are significantly wider than the ideal tetrahedral angle (109.47°) The coordination bond distances and angles agree well with the literature values of Ru complexes.[28]

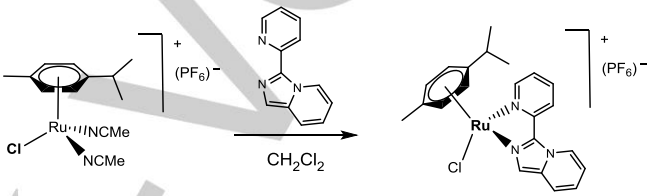

Scheme 5. Synthesis of complex **17**

Contrary to the expected behaviour, some of the structures discussed above show twisted indolizine ligands. The twist angles, defined as the dihedral angle between the mean planes of the pyridine and imidazo rings, have been calculated with the Mercury program and are gathered in the Table 3. Examining the packing of the different structures, it is observed that the indolizine ligand is almost planar when is π-stacked with another indolizine from a neighboring molecule. To support the idea that the twisting is related to the packing and not to electronic effects, an optimization of the structure for the Ni complex **1** was performed at the B3LYP level, using the LANL2DZ basis set for the Ni, P and S atoms, and 6-31G(d,p) for the rest of elements. The optimization was started at the geometry of the X-ray structure, with a twist angle of approximately 20º, and the minimum was found with a much less twisted indolizine ligand (7º).

Table 1. Twist angles between the pyridine and imidazo rings of the Py-indz complexes.

Complexes	1	2	3	4	6	7	8	9
Twist angle (°)	19.93	2.67	9.29	9.10[a]	9.44	0.38	7.23	22.39
Complexes	10	11	12	13	14	15	16	17
Twist angle (°)	3.52	4.81	2.69	12.07	3.77	5.00	9.11	9.10

[a] Calculated as an average of the twist angle of the three Py-indz ligands

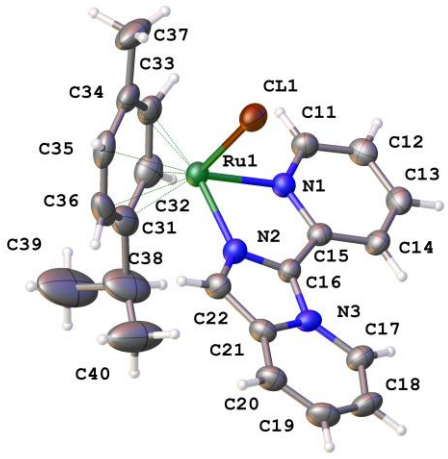

Figure 10. Cation of compound **17**. Selected bond lengths (Å) and angles (º): Ru(1)-N(1) 2.104(4), Ru(1)-N(2) 2.061(4), Ru(1)-Cl(1) 2.394(1), Ru(1)-Cent 1.676(5), N(1)-Ru(1)-N(2) 79.49(9), Cl(1)-Ru(1)-N(I) 85.85(11), Cl(1)-Ru(1)-N(2) 84.66(12), Cl(1)-Ru(1)-Cent 128.27(2), N(1)-Ru(1)-Cent 131.29(2), N(2)-Ru(1)-Cent 132.15(2).

Conclusions

A variety of new complexes has been prepared using main group and transition metal moieties and the Py-indz ligand, and their structures have been fully characterized by spectroscopic methods and X-ray crystallography. In some cases, the structures can be induced by stoichiometry and complexes can be obtained with one, two or three molecules of the ligand. The twist angle between the imidazo and pyridine rings of the ligand is related to the packing mode of the structures, when two Py-indz ligands from neighbouring molecules are π-stacked, these ligands are approximately planar, while when the π-stacking is missing the twisting is significant. The ability of Py-indz to act as ligand towards metals in very different environments has been fully demonstrated. The Py-indz ligand behaves as a chelating ligand with similar electronic properties to the classical 2,2'-bipyridine or 1,10-phenanthroline. In this way, a value of 12554 for Δo was found in tris-chelate complexes of Py-indz with Ni(II), while Δo ranges from 12650 to 12700 for the corresponding bipy or phen Ni(II) complexes.Main Text Paragraph.

Experimental Section

Materials and general methods: some operations were performed under an atmosphere of dry nitrogen using Schlenk and vacuum techniques. Solvents, ligands and other reagents were purchased and used without purification unless otherwise stated. 3-(Pyridin-2-yl)imidazo[1,5-a]pyridine (Py-indz) was prepared using the method reported by us.[**¡Error! Marcador no definido.**] The precursors were prepared following the literature: $[Ni(S_2P(OEt)_2)_2]$, [29a] $[Ni(S_2COEt)_2]$,[29b] $[Ni(acac)_2(MeOH)_2]$, [29c] $[Zn(S_2P(OEt)_2)_2]$, [22a] $[Cd(S_2P(OEt)_2)_2]$, [23a] $[Cu(NCMe)_2(PPh_3)_2]BF_4$,[30] $[MBr(CO)_5]$ M= Mn,[31] Re,[32] $[RuCl(p\text{-}cymene)(NCMe)_2]PF_6$ was prepared from $[RuCl_2(p\text{-}cymene)_2]$, [33] with NH_4PF_6 and stirring 12 hours in acetonitrile. All others agents were obtained from the usual commercial suppliers, and used as received. Kieselguhr (diatomaceous earth, Merck) was used for filtration. IR spectra in solution were recorded with a Perkin Elmer Spectrum RX I FT-IR instrument, using cells with CaF_2 windows. All NMR solvents were stored over molecular sieves and degassed prior to use. NMR experiments were measured on an Agilent MR400 and Agilent DDR2 500 spectrometers. Chemical shift values are given in ppm using the residual solvent signal as an internal reference. The splitting of proton resonances in the reported 1H NMR data is defined as s = singlet, d = doublet, t = triplet, q = quartet, m = multiplet. 2D experiments such as $^1H-^1H$ gCOSY, $^1H-^1H$ NOESY, $^1H-^{13}C$ gHSQC, and $^1H-^{13}C$ gHMBC were recorded using standard pulse sequences. All NMR data processing was carried out using MestReNova, version 9.1.0. The magnetic moments were calculated from magnetic susceptibilities which were measured in Unidade de Magnetosusceptibilidade of Santiago de Compostela University. HRMS measurement (High Resolution Mass Spectroscopy) was performed in the Laboratorio de Técnicas Instrumentales of Valladolid University. Elemental analyses were performed on a Perkin-Elmer 2400B microanalyzer.

Computational details: all computations were carried out using the GAUSSIAN09 package,[34] in which the hybrid method B3LYP was applied with the Becke three-parameter exchange functional,[35] and the Lee-Yang-Parr correlation functional.[36] Effective core potentials (ECP) and their associated double-z LANL2DZ basis set were used for the heavy atoms (Ni, P, S, Sn, I).[37] The light elements (O, N, C, and H) were described with the 6-31G** basis.[38] Geometry optimizations were performed under no symmetry restrictions, using initial coordinates derived from X-ray data of the same complexes, and frecuency analyses were performed to ensure that a minimum structure with no imaginary frecuencies was achieved in each case.

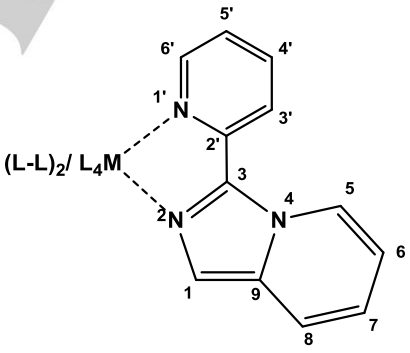

Scheme 6. Numbering scheme for the protons and carbons of Py-indz ligand.

$Ni(S_2P(OEt)_2)_2$(Py-indz)] (1): to a violet solution of $[Ni(S_2P(OEt)_2)_2]$ (0.429 g, 1 mmol) in dichloromethane was added Py-indz (0.195 g, 1 mmol) and the mixture was stirred overnight. The resulting solution was concentrated in vacuo to afford compound **1** as a green microcrystalline solid. Yield 0.582 g, 93%. Analysis calculated for $C_{20}H_{29}N_3Ni_1O_4P_2S_4$: C 38.48, H 4.68, N 6.73. Found: C 39.06, H 4.48, N 6.40. μeff (293K): 2.78 BM. Crystals of **1** suitable for X-ray analysis were grown from CH_2Cl_2–hexane at −20 °C.

$[Ni(S_2COEt)_2$(Py-indz)] (2): to a black solution of $[Ni(S_2COEt)_2]$ (0.429 g, 1 mmol) in dichloromethane was added Py-indz (0.195 g, 1 mmol) and the mixture was stirred overnight. The resulting solution was concentrated in vacuo to afford compound **2** as a green microcrystalline solid. Yield 0.472 g, 95%. Analysis calculated for $C_{18}H_{19}N_3Ni_1O_2S_4$: C

43.56, H 3.86, N 8.47. Found: C 43.16, H 3.72, N 8.23. μeff (293K): 2.40 BM. Crystals of **2** suitable for X-ray analysis were grown from CH_2Cl_2–hexane at −20 °C.

[Ni(acac)$_2$(Py-indz)] (3): to a blue pale solution of [Ni(acac)$_2$(MeOH)$_2$] (0.321 g, 1 mmol) in tetrahydrofuran was added Py-indz (0.195 g, 1 mmol) and the mixture was stirred overnight. The resulting solution was concentrated in vacuo to afford compound **3** as a green microcrystalline solid. Yield 0.413 g, 91%. Analysis calculated for $C_{22}H_{23}N_3Ni_1O_4$: C 58.44, H 5.13, N 9.29. Found: C 58.32, H 5.02, N 9.22. μeff (293K): 2.78 BM. Crystals of **3** suitable for X-ray analysis were grown from THF–hexane at −20 °C.

[Ni(Py-indz)$_3$](PF$_6$)$_2$ (4): to a 10 mL aqueous solution of $Ni(ClO_4)_2{\cdot}6H_2O$ (0.366 g, 1 mmol) was added 10 mL of Py-indz (0.585 g, 3 mmol) in dichloromethane with stirring and NH_4PF_6 (0.326 g, 2 mmol). The green solution was stirred 6 hours and then an extraction with dichloromethane was done (3 × 15 mL), followed by drying over $MgSO_4$. Slow evaporation at reduced pressure gave compound **4** as a microcrystalline solid. Yield 0.700 g, 75%. Analysis calculated for $C_{36}H_{27}N_9Ni_1P_2F_{12}$: C 46.28, H 2.91, N 13.49. Found: C 46.10, H 2.72, N 13.52. μeff (20K): 2.90 BM. Crystals of **4** suitable for X-ray analysis were grown from CH_2Cl_2-ether at −20 °C.

[Fe(Py-indz)$_3$](PF$_6$)$_2$ (5): a similar procedure to that described for **4** was used to obtain **5**, using $(NH_4)_2Fe(SO_4){\cdot}6H_2O$ (0.392 g, 1 mmol), and Py-indz (0.585 g, 3 mmol). The red compound **5** precipitated after NH_4PF_6 (0.326 g, 2 mmol) was added. Extraction with dichloromethane (3 × 15 mL), followed by drying over $MgSO_4$, filtering through Kieselghur and slow evaporation at reduced pressure gave compound **5** as a microcrystalline solid. Yield 0.822 g, 88%. Analysis calculated for $C_{36}H_{27}FeN_9P_2F_{12}$: C 46.42, H 2.92, N 13.53. Found: C 46.40, H 2.84, N 13.71. HRMS (ESI-TOF) m/z= 320.612 $[M\text{-}2PF_6]^{2+}$, calcd. 320.586 for $C_{36}H_{27}N_9Fe$. ^{1}H NMR (400 MHz, Me_2CO-d_6): δ 9.27-9.18 (m, 2H, $H^5{}_{isomerA}$, $H^5{}_{isomerB}$), 8.76-8.64 (m, 2H, $H^{6'}{}_A$, $H^{6'}{}_B$), 8.24-8.15 (m, 2H, $H^{5'}{}_A$, $H^{5'}{}_B$), 7.98-7.82 (m, 2H, $H^{3'}{}_A$, $H^{3'}{}_B$), 7.82-7.70 (m, 2H, $H^8{}_A$, $H^8{}_B$), 7.41 – 7.30 (m, 2H, $H^{4'}{}_A$, $H^{4'}{}_B$), 7.30-7.23 (m, 4H, $H^7{}_A$, $H^7{}_B$, $H^1{}_A$, $H^1{}_B$), 7.23 – 7.14 (m, 2H, $H^6{}_A$, $H^6{}_B$) ppm. ^{13}C NMR (101 MHz, Me_2CO-d_6): δ 155.77, 155.74 (s, $C^{3'}{}_A$, $C^{3'}{}_B$); 151.80, 151.70 (s, $C^{2'}{}_A$, $C^{2'}{}_B$); 138.12, 138.04 (s, $C^{5'}{}_A$, $C^{5'}{}_B$); 136.17, 136.02 (s, $C^3{}_A$, $C^3{}_B$); 135.85, 135.72 (s, $C^9{}_A$, $C^9{}_B$); 124.86, 124.73 (s, $C^6{}_A$, $C^6{}_B$); 123.70, 123.54 (s, $C^{4'}{}_A$, $C^{4'}{}_B$); 123.29, 123.23 (s, $C^5{}_A$, $C^5{}_B$); 122.89, 122.72 (s, $C^1{}_A$, $C^1{}_B$); 120.48, 120.10 (s, $C^{6'}{}_A$, $C^{6'}{}_B$); 117.91, 117.86 (s, $C^8{}_A$, $C^8{}_B$); 116.43, 116.43 (s, $C^7{}_A$, $C^7{}_B$) ppm. ^{31}P NMR (162 MHz, Me_2CO-d_6): δ -144.31 ppm.

[Mn$_2$Cl$_4$(Py-indz)$_2$] (6): to a colorless solution of anhydrous $MnCl_2$ (0.126 g, 1 mmol) in methanol was added Py-indz (0.195 g, 1 mmol). After 2 hours with stirring, the solution changed to yellow and evaporated to dryness. The residue was dissolved in dichloromethane and filtered and the resulting solution was concentrated to give the yellow compound **6** as a microcrystalline solid. Yield 0.610 g, 95%. μeff: 5.65 BM. Analysis calculated for $C_{24}H_{18}Cl_4Mn_2N_6$: C 44.89, H 2.83, N 13.09. Found: C 44.77, H 2.91, N 13.26. Orange crystals of **6** suitable for X-ray analysis were grown from CH_2Cl_2–hexane at room temperature.

[MnCl$_2$(Py-indz)$_2$] (7): compound **7** was prepared as described above for **6**, using anhydrous $MnCl_2$ (0.126 g, 1 mmol) and Py-indz (0.390 g, 2 mmol).Yield 0.502 g, 97%. μeff (293K): 5.84 BM. Analysis calculated for $C_{24}H_{18}N_6Cl_2Mn_1$: C 55.83, H 3.51, N 16.28. Found: C 55.62, H 3.11, N 16.18. Yellow crystals of **7** suitable for X-ray analysis were grown from CH_2Cl_2–hexane at room temperature.

[Zn(S$_2$P(OEt)$_2$)$_2$ (Py-indz)] (8): to a colorless solution of $[Zn(S_2P(OEt)_2)_2]$ (0.436 g, 1 mmol) in dichloromethane was added Py-indz (0.195 g, 1 mmol) and the mixture was stirred overnight. The resulting solution was concentrated in vacuo to afford compound **8** as a yellow microcrystalline solid. Yield 0.612 g, 97%. Analysis calculated for $C_{20}H_{29}N_3O_4P_2S_4Zn_1$: C 38.07, H 4.63, N 6.66. Found: C 38.17, H 4.48, N 6.42. Crystals of **8** suitable for X-ray analysis were grown from CH_2Cl_2–hexane at −20 °C. ^{1}H NMR (400 MHz, Me_2CO-d_6): δ 9.19 (d, J = 6.4 Hz, 1H, H^5), 8.95 (d, J = 5.03 Hz 1H, $H^{6'}$), 8.55 (d, J = 8.2 Hz, 1H, $H^{3'}$), 8.31 (td, J = 7.9, 1.7 Hz, 1H, $H^{4'}$), 8.11 (s, 1H, H^1), 8.08 – 7.99 (d, J = 7.02 Hz, 1H, H^8), 7.72 (ddd, J = 7.7, 5.1, 1.0 Hz, 1H, $H^{5'}$), 7.31 – 7.20 (m, 2H, H^6, H^7), 3.96 (dq, J = 9.6, 7.1 Hz, 8H, CH_2), 1.14 (t, J = 7.1 Hz, 12H, CH_3) ppm. ^{13}C NMR (101 MHz, Me_2CO-d_6): δ 150.81 (s, $C^{6'}$), 145.09 (s, $C^{2'}$), 141.41 (s, $C^{4'}$), 137.81 (s, C^3), 135.13 (s, C^9), 125.12 (s, $C^{5'}$), 124.71 (s, C^5), 123.21 (s, C^7), 122.02 (s, C^1), 120.94 (s, $C^{3'}$), 120.71 (s, C^8), 118.07(s, C^6), 110.93, 62.92 (s, CH_2), 16.17 (s, CH_3) ppm. ^{31}P NMR (162 MHz, Me_2CO-d_6): δ 103.21 ppm.

[Cd(S$_2$P(OEt)$_2$)$_2$ (Py-indz)] (9): to a colorless solution of $[Cd(S_2P(OEt)_2)_2]$ (0.482 g, 1 mmol) in dichloromethane was added Py-indz (0.195 g, 1 mmol) and the mixture was stirred overnight. The resulting solution was concentrated in vacuo to afford compound **9** as a yellow microcrystalline solid. Yield 0.663 g, 98%. Analysis calculated for $C_{20}H_{29}Cd_1N_3O_4P_2S_4$: C 35.43, H 4.31, N 6.20. Found: C 35.52, H 4.28, N 6.32. Crystals of **9** suitable for X-ray analysis were grown from CH_2Cl_2–hexane at −20 °C. ^{1}H NMR (500 MHz, $CDCl_3$): δ 9.18 (d, J = 7.0 Hz, 1H, $H^{6'}$), 8.68 (d, J = 7.1 Hz, 1H, $H^{5'}$), 8.01-7.97 (m, 2H, $H^{3'}$ y $H^{4'}$) 7,99 (s, 1H, H^1), 7.67 (d, J = 8.6 Hz, 1H, H^8), 7.42 (ddd, J = 7.3, 5.0, 1.3 Hz, 1H, $H^{5'}$), 7.02 – 6.98 (m, 1H, H^7), 6.96 (td, J = 6.9, 1.4 Hz, 1H, H^6), 4.20 (dq, J = 9.5, 7.1 Hz, 8H, CH_2), 1.33 (t, J = 6.9Hz, 12H, CH_3) ppm. ^{13}C NMR (126 MHz, $CDCl_3$): δ 150.53 (s, $C^{6'}$), 144.40 (s, $C^{2'}$), 139.01 (s, $C^{4'}$), 134.12 (s, C^3), 133.94 (s, C^9), 123.82 (s, $C^{5'}$), 122.70 (s, C^5), 121.37 (s, C^7), 121.34 (s, $C^{3'}$), 120.00 (s, C^8), 119.49 (s, C^1), 116.60 (s, C^6), 63.74-63.69 (d, CH_2), 16.18-16.11 (d, CH_3). ^{31}P NMR (162 MHz, $CDCl_3$) δ 108.11 ppm.

[SnI$_4$(Py-indz)] (10): to an orange solution of SnI_4 (0.626 g, 1 mmol) in dichloromethane was added Py-indz (0.195 g, 1 mmol) with stirring. After two hours a red precipitate appeared. The solution was filtered with a fritted funnel and the crude was washed three times with hexane. Yield 0.790 g, 96%. Analysis calculated for $C_{12}H_9I_4N_3Sn_1$: C 17.54, H 1.10, N 5.12. Found: C 17.62, H 1.19, N 5.07. Suitable crystals of **10** for X-ray analysis appeared at the wall of the vial after two days at room temperature by layering a solution of SnI_4 in methanol with another solution of the Py-indz ligand in ether.

[PhSnCl$_3$(Py-indz)] (11): to a light yellow solution of $PhSnCl_3$ (0.302 g, 1 mmol) in dichloromethane was added Py-indz (0.195 g, 1 mmol) with stirring. After two hours a yellow precipitate appeared. The solution was filtered with a fritted funnel and the crude was washed three times with dichloromethane. Yield 0.400 g, 80%. Analysis calculated for $C_{18}H_{14}Cl_3N_3Sn_1$: C 43.47, H 2.84, N 8.45. Found: C 43.10, H 2.75, N 8.33. Crystals of **11** suitable for X-ray analysis were grown from MeOH-ether at −20 °C. ^{1}H NMR (400 MHz, acetone) δ 9.51 (d, J = 6.4 Hz, 1H, $H^{6'}$), 9.30 (d, J = 6.5 Hz, 1H, H^5), 8.89 (d, J = 8.2 Hz, 1H, $H^{3'}$), 8.62 (t, J = 7.35 Hz, 1H, $H^{4'}$), 8.38 (s, 1H, H^1), 8.25 – 8.18 (m, 1H, H^8), 8.06 (t, J = 6.5 Hz, 1H, $H^{5'}$), 7.56 – 7.45 (m, 2H, $H^{7,6}$), 7.27 – 7.08 (m, 5H, (H)Ph). ^{13}C NMR (101 MHz, acetone) δ 145.65 (s, $C^{6'}$), 137.32 (s, $C^{4'}$), 128.83 (s, Ph), 128.0 (s, Ph), 126.52 (s, C^5), 126.00 (s, $C^{5'}$), 124.78 (s, $C^{3'}$), 121.72 (s, C^1), 120.45 (s, C^7), 119.11 (s, C^8), 117.24 (s, C^6) ppm.

[^{n}Bu$_2$SnCl$_2$(Py-indz)] (12): Bu^nSnCl_2 (0.304 g, 1 mmol) and Py-indz (0.195 g, 1 mmol) were stirred overnight in dichloromethane. Slow evaporation at reduced pressure gave compound **12** as a microcrystalline solid. Yield 0.790 g, 94%. Analysis calculated for $C_{20}H_{27}Cl_2N_3Sn_1$: C 48.16, H 5.45, N 8.42. Found: C 48.23, H 5.19, N 8.07. Yellow crystals of **12** suitable for X-ray analysis were grown from CH_2Cl_2-ether at room temperature. ^{1}H NMR (500 MHz, -50ºC, Nitromethane-d_3) δ

9.17 (s, 1H, H^5), 8.97 (s, 1H, H^6), 8.41 (s, 1H, $H^{3'}$), 8.32 (s, 1H, $H^{4'}$), 8.10 (s, 1H, H^1), 7.94 (s, 1H, H^8), 7.72 (s, 1H, $H^{5'}$), 7.28 (d, J = 8.5 Hz, 1H, H^7), 7.25 (s, 1H, H^6), 1.47 (m, 4H, CH_2-Sn), 1.21 (m, 4H, -CH_2-), 1.04 (m, 4H, CH_2-Me), 0.62 (m, 6H, CH_3). ^{13}C NMR (101 MHz, -50ºC, Nitromethane-d_3): δ 148.65 (s, C^5), 140.76 (s, $C^{4'}$), 124.68 (s, $C^{5'}$), 123.94 (s, $C^{6'}$), 123.16 (s, C^7), 120.45 (s, $C^{3'}$), 119.55 (s, C^1), 119.55 (s, C^8), 117.44 (s, C^6), 29.33 (s, CH_2-Sn), 28.19 (s, -CH_2-), 25.91(s, CH_2-Me), 12.82 (s, CH_3) ppm.

[Cu(PPh$_3$)$_2$(Py-indz)]BF$_4$ (13): compound **13** was prepared with a similar procedure to **8** by using [Cu(NCMe)$_2$(PPh$_3$)$_2$]BF$_4$ (0.757 g, 1 mmol) and Py-indz (0.195 g, 1 mmol) in dichloromethane with stirring. Yield 0.790 g, 94%. Analysis calculated for $C_{48}H_{39}Cu_1N_3P_2B_1F_4$: C 66.49, H 4.19, N 4.85. Found: C 66.07, H 4.53, N 4.78. Light yellow crystals of **13** suitable for X-ray analysis were grown from CH_2Cl_2-ether at room temperature. ^{1}H NMR (400 MHz, Me_2CO-d_6) δ 8.99 (d, J = 6.5 Hz, 1H, H^5), 8.62 (d, J = 5.0 Hz, 1H, H6'), 8.45 (d, J = 8.2 Hz, 1H, H3'), 8.16 (t, J = 7.9 Hz, 1H, H4'), 7.86 (s, 1H, H^1), 7.82 – 7.75 (m, 1H, H^8), 7.41 (m, 1H, $H^{5'}$), 7.41 (d, J = 7.3 Hz, 6H, Ph-H^{para}), 7.28 (dd, J = 14.6, 7.4 Hz, 24H, Ph-$H^{ortho,meta}$), 7.22 – 7.12 (m, 2H, $H^{6,7}$). ^{13}C NMR (101 MHz, Me_2CO-d_6) δ 150.85 (s, $C^{6'}$), 145.38 (s, $C^{2'}$), 138.81 (s, $C^{4'}$), 135.12 (s, $C^{3'}$), 134.58 (s, C^9), 133.15 (s, CH^{ortho}), 130.17 (s, CH^{para}), 128.76 (s, CH^{meta}), 123.88 (s, $C^{5'}$), 123.33 (s, C^5), 122.13 (s, C^7), 121.26 (s, C^1), 120.66 (s, $C^{3'}$), 119.06 (s, C^8), 116.42 (s, C^6). ^{31}P NMR (202 MHz, Me_2CO-d_6): δ -99.97 ppm.

[MnBr(CO)$_3$(Py-indz)] (14): to a solution of Py-indz (0.195 g, 1 mmol) in hexane (20 mL) was added [MnBr(CO)$_5$] (0.275 g, 1 mmol) and the mixture was refluxed for 2 hours under nitrogen atmosphere. After that time a yellow solid was formed, which was filtered off, washed with hexane (3 × 15 mL) and dried in vacuo. Yield 0.213 g, 78%. Analysis calculated for $C_{15}H_9Br_1Mn_1N_3O_3$: C 43.51, H 2.19, N 10.15. Found: C 43.62, H 2.11, N 10.72. IR (THF, cm^{-1}), ν(CO): 2022 vs, 1934 s, 1911 s. Yellow crystals of **14** suitable for X-ray analysis were grown from CH_2Cl_2-ether at room temperature. ^{1}H NMR (500 MHz, Me_2CO-d_6) δ 9.28 (d, J = 5.18 Hz, 1H, $H^{6'}$), 9.06 (d, J = 6.8 Hz, 1H, H^5), 8.50 (d, J = 7.9 Hz, 1H, $H^{3'}$), 8.28 (s, 1H, H^1), 8.21 (m, 1H, $H^{4'}$), 7.98 (d, J = 9.4 Hz, 1H, H^8), 7.59 (m, 1H, $H^{5'}$), 7.29 (s m, 1H, $H^{5'}$), 7.29 (t, J = 7.7 Hz, 1H, H^7), 7.22 (m, 1H, H^6) ppm. ^{13}C NMR (126 MHz, Me_2CO-d_6) δ 166.10 (s, CO), 154.67 (s, $C^{6'}$), 147.54 (s, $C^{2'}$), 138.78 (s, $C^{4'}$), 135.94 (s, C^3), 134.34 (s, C^9), 124.18 (s, C^1), 123.67 (s, $C^{5'}$), 123.27 (s, C^5), 122.57 (s,C^7), 120.20 (s, $C^{3'}$), 118.55 (s, C^8), 116.55 (s, C^6) ppm.

[ReBr(CO)$_3$(Py-indz)] (15): to a solution of Py-indz (0.195 g, 1 mmol) in hexane (20 mL) was added [ReBr(CO)$_5$] (0.275 g, 1mmol) and the mixture was refluxed for 8 hours under nitrogen atmosphere. After that time a yellow solid was formed, which was filtered off, washed with hexane (3 × 15 mL) and dried in vacuo. Yield 0.463 g, 85%. Analysis calculated for $C_{15}H_9Br_1Re_1N_3O_3$: C 33.04, H 1.66, N 7.71. Found: C 33.29, H 1.68, N 7.90. IR (THF, cm^{-1}), ν(CO): 2018 vs, 1917 s, 1891 s. Yellow crystals of **15** suitable for X-ray analysis were grown from CH_2Cl_2-ether at room temperature. ^{1}H NMR (400 MHz, Me_2CO-d_6) δ 9.16 (d, J = 6.8 Hz, 1H, H^5), 9.12 (d, J = 5.6 Hz, 1H, $H^{6'}$), 8.63 (d, J = 8.3 Hz, 1H, $H^{3'}$), 8.31 (td, J = 8.0, 1.7 Hz, 1H, $H^{4'}$), 8.17 (s, 1H, H^1), 8.01 (d, J = 9.0 Hz, 1H, H^8), 7.62 (dd, J = 7.7, 5.6 Hz, 1H, $H^{5'}$), 7.40 – 7.33 (m, 1H, H^7), 7.31 (td, J = 6.9, 1.5 Hz, 1H, H^6) ppm. ^{13}C NMR (101 MHz, Me_2CO-d_6) δ 166.10 (s, CO), 154.24 (s, $C^{6'}$), 148.09 (s, $C^{2'}$), 139.63 (s, $C^{4'}$), 138.85 (s, C^3), 135.02 (s, C^9), 124.59 (s, $C^{5'}$), 123.77 (s, C^1), 123.42 (s, C^5), 123.26 (s, C^7), 121.02 (s, $C^{3'}$), 118.97 (s, C^8), 117.36 (s, C^6) ppm.

[Mo(CO)$_4$(Py-indz)] (16): to a solution of Py-indz (0.195 g, 1 mmol) in toluene (20 mL) was added [Mo(CO)$_6$] (0.264 g, 1mmol) and the mixture was refluxed for 6 hours under nitrogen atmosphere. After that time the solution changed to yellow-orange. Toluene was evaporated and the crude was dissolved in dichloromethane and filtered off. Hexane was added to precipitate complex **16** as a microcrystalline yellow solid. Yield 0.356 g, 88%. Analysis calculated for $C_{16}H_9Mo_1N_3O_4$: C 47.66, H 2.25, N 10.42. Found: C 47.52, H 2.19, N 10.26. IR (THF, cm^{-1}), ν(CO): 2010 vs, 1895 vs, 1878 s, 1838 s. Yellow crystals of **16** suitable for X-ray analysis were grown from CH_2Cl_2-ether at -20°C. ^{1}H NMR (400 MHz, Me_2CO-d_6) δ 9.13 (ddd, J = 5.5, 1.6, 0.9 Hz, 1H, $H^{6'}$), 9.08 (dd, J = 7.2, 1.0 Hz, 1H, H^5), 8.52 (dt, J = 8.3, 1.0 Hz, 1H, $H^{3'}$), 8.19 (ddd, J = 8.2, 7.5, 1.7 Hz, 1H, $H^{4'}$), 8.02 (d, J = 0.9 Hz, 1H, H^1), 7.94 (dt, J = 9.2, 1.4 Hz, 1H, H^8), 7.51 (ddd, J = 7.6, 5.4, 1.1 Hz, 1H, $H^{5'}$), 7.27 (td, J = 6.7, 1.4 Hz, 1H, H^7), 7.19 (td, J = 6.9, 1.4 Hz, 1H, H^6). ^{13}C NMR (101 MHz, Me_2CO-d_6) δ 165.10 (s, CO), 153.78 (s, $C^{6'}$), 147.44 (s, $C^{2'}$), 138.31 (s, $C^{4'}$), 136.0 (s, C^3), 134.40 (s, C^9), 124.27 (s, C^1), 123.45 (s, C^5), 123.01 (s, $C^{5'}$), 122.45 (s, C^7), 120.46 (s, $C^{3'}$), 118.54 (s, C^8), 116.28 (s, C^6) ppm.

[RuClp-cym(Py-indz)]PF$_6$ (17): Py-indz (0.195 g, 1 mmol) was added to a [RuClp-cym(NCMe)$_2$]PF$_6$ (0.474 g, 1 mmol) solution in dichloromethane under nitrogen atmosphere. After two hours, the colour changed from orange to yellow. The solution was concentrated to give a yellow microcrystalline solid which was recrystallized from CH_2Cl_2–hexane. Yield 0.472 g, 95%. Analysis calculated for $C_{22}H_{23}Cl_1F_6N_3P_1Ru_1$: C 43.25, H 3.80, N 6.88. Found: C 43.16, H 3.92, N 6.52. Orange crystals of **17** suitable for X-ray analysis were grown from CH_2Cl_2-ether at room temperature. ^{1}H NMR (400 MHz, Me_2CO-d_6) δ 9.63 (d, J = 5.6 Hz, 1H, $H^{6'}$), 9.11 (d, J = 7.0 Hz, 1H, H^5), 8.66 (s, 1H, H^1), 8.56 (d, J = 8.1 Hz, 1H, $H^{3'}$), 8.29 (t, J = 7.8 Hz, 1H, $H^{4'}$), 8.01 (d, J = 8.9 Hz, 1H, H^8), 7.64 (t, J = 6.7 Hz, 1H, $H^{5'}$), 7.44 – 7.35 (m, 1H, H^7), 7.30 (t, J = 6.9 Hz, 1H, H^6), 6.23 (dd, J = 12.5, 6.1 Hz, 2H, ArH), 6.00 (dd, J = 12.0, 6.0 Hz, 2H, ArH), 2.77 (s, 1H, CH_iPr), 2.27 (s, 3H, CH_3Ar), 1.13 (dd, J = 10.9, 6.7 Hz, 6H, $CH_{3i}Pr$). ^{13}C NMR (101 MHz, acetone) δ 157.44 (s, $C^{6'}$), 140.52 (s, $C^{4'}$), 135.20 (s, $C^{6'}$), 126.28 (s, C^1), 125.22 (s, $C^{5'}$), 124.62 (s, C^7), 124.47 (s, C^5), 121.68 (s, $C^{3'}$), 119.46 (s, C^8), 118.26 (s, C^6), 105.78 (s, ArC^*), 103.06 (s, ArC^*), 86.55 (s, ArCH), 85.84 (s, ArCH), 85.41 (s, ArCH), 84.15 (s, ArCH), 31.87 (s, CH_iPr), 22.47 (s, $CH_{3i}Pr$), 22.09 (s, $CH_{3i}Pr$), 18.80 (s, CH_3Ar).

X-Ray Diffraction Study of 1 2, 3, 4, 6, 7, 8, 9, 10, 11, 12, 13, 14, 15, 16 and 17: diffraction data were collected using an Oxford Diffraction Supernova diffractometer, equipped with an Atlas CCD area detector and a four-circle kappa goniometer. For the data collection Mo or Cu micro-focus sources with multilayer optics were used. Data integration, scaling and empirical absorption correction was carried out using the CrysAlis Pro program package. [39] The structure was solved using direct methods and refined by Full-Matrix-Least-Squares against F^2 with SHELX [40] under OLEX2. [41] The non-hydrogen atoms were refined anisotropically and hydrogen atoms were placed at idealised positions and refined using the riding model. Graphics were made with OLEX2 and MERCURY. [42] Crystal data, particular details and CCDC reference numbers are given in Table 4.

[1] C. M. Alvarez, L. Alvarez-Miguel, R. Garcia-Rodriguez, D. Miguel, *Dalton Trans*. **2012**, *41*, 7041-7046.

[2] R. Grigg, P. Kennewell, V. Savic, V. Sridharan, *Tetrahedron*, **1992**, *47*, 10423-10430.

[3] a) J. M.Crawford, M. Paoletti, *Tetrahedron Lett.*, **2009**, *50*, 4916-4918. b) J. Wang, R. Mason, K. VanDerveer, D. Feng, X. R. Bu, *J.Org.Chem.*, **2003**, *68*, 5415-5418. c) J. Wang, L. Jr Dyers, R. Mason, P. Amoyaw, X. R. Bu, *J.Org.Chem*., **2005**, *70*, 2353-2356. d) S. A. Siddiqui, T. M. Potewar, R. J. Lahoti, K. V. Srinivasan, *Synthesis*, **2006**, *17*, 2849-2854. e) S. V. Arvapalli, G. Chen, S. Kosarev, E. M. Tan, D. Xie, L. Yet, *Tetrahedron Lett.*, **2010**, *51*, 284-286. f) M. Ostermeier, C. Limberg, B. Ziemer, V. Karunakaran, *Angew. Chem.*, Int. Ed., **2007**, *46*, 5329-5331.

[4] a) F. Shibahara, R. Sugiura, E. Yamaguchi, A. Kitagawa,; T. J. Murai, *Org. Chem*., **2009**, *74*, 3566-3568. b) F. Shibahara, E. Yamaguchi, A. Kitagawa, A. Imai, T. Murai, *Tetrahedron*, **2009**, *65*, 5062-5073.

[5] F. Shibahara, A. Kitagawa, E. Yamaguchi, T. Murai, *Org. Lett.*, **2006**, *8*, 5621-5624.

[6] F. Palacios, C. Alonso, G. Rubiales, *Tetrahedron*, **1995**, *51*, 3683-3690.

[7] I. R. Lahoz, C. Sicre, A. Navarro-Vazquez, C. Silva-López, M. M. Cid, *Org. Lett.*, **2009**, *21*, 4802-4805.

[8] J. T. Hutt, Z. D. Aron, *Org. Lett.*, **2011**, *13*, No. 19, 5256-5259.

[9] a) M. E. Bluhm, V. Ciesielski, H. Görls, M. Döring, *Angew. Chem., Int. Ed.* **2002**, *41*, 2962-2965. b) V. Bluhm, M. Ciesielski, H. Görls, O. Walter, M. Döring, *Inorg. Chem.* **2003**, *42*, 8878-8885. c) Y. Chen, L. Li, Y. Cao, J. Wu, Q. Gao, Y. Li, H. Hu, W. Liu, Y. Liu, Z. Kang, J. Li, *Cryst. Eng. Comm.* **2013**, *15*, 2675-2681.

[10] M. E. Bluhm, C. Folli, D. Pufky, M. Kröger, O. Walter; M. Döring, *Organometallics* **2005**, *24*, 4139-4152.

[11] A. G. J. Ligtenbarg, A. L. Spek, R. Hage, B. L. Feringa, *J. Chem. Dalton Trans*. **1999**, 659-662.

[12] G. Volpi, C. Garino, L. Salassa, J. Fiedler, K. I. Hardcastle, R. Gobetto, C. Nervi, *Chem-Eur. J*. **2009**, *15*, 6415-6427.

[13] a) C. Garino, T. Ruiu, L. Salassa, A. Albertino, G. Volpi, C. Nervi, R. Gobetto, K. I. Hardcastle, *Eur. J. Inorg.Chem*. **2008**, *2008*, 3587-3591. b) L. Salassa, C. Garino, A. Albertino, G. Volpi, C. Nervi, R. Gobetto, K. I. Hardcastle, *Organometallics* **2008**, *27*, 1427-1435.

[14] M. Hakimia, Z. Mardania, K. Moeinia, F. Mohrb, E. Schuhb, H. Z. Vahedia, *Naturforsch* **2012**, *67b*, 452-458.

[15] T. Murai, E. Nagaya, K. Miyahara, F. Shibahara, T. Maruyama, *Chemistry Letters* **2013**, *42*, 828-830.

[16] M.Li, Y. Xie, Y. Ye, Y. Zou, H. Jiang, W. Zeng, *Org. Lett.* **2014**, *16*, 6232-6235.

[17] J.-S. Choi, J. J. Braymer, S. K. Park, S. Mustafa, J. Chae, M. H. Lim, *Metallomics* **2011**, *3*, 284-291.

[18] Use in FET (Field Effect Transistor): a) H. Nakamura, H. Yamamoto, PCT Int. Appl. WO 2005043630; *Chem. Abstr*. **2005**, *142*, 440277. OLED: (Organic Light-Emitting Diodes); b) M. Nakatsuka, T. Shimamura, Jpn. Kokai Tokkyo Koho JP 2001035664; *Chem. Abstr*. **2001**, *134*, 93136; c) D. Kitazawa, G. Tominaga, A. Takano, Jpn. Kokai Tokkyo Koho JP 2001057292.

[19] Bioactivity of imidazo[1,5-a]pyridines: a) D. Kim, L. Wang, J. Hale, C. L. Lynch, R. J. Budhu, M. MacCoss, S. G. Mills, L. Malkowitz, S. L. Gould, J. A. DeMartino, M. S. Springer, D. Hazuda, M. Miller, J. Kessler, R. C. Hrin, G. Carver, A. Carella, K. Henry, J. Lineberger, W. A. Schelif, E. A. Emini, *Bioorg. Med. Chem. Lett* **2005**, *15*, 2129-2134. b) L. J. Browne, C. Gude, H. Rodriguez, R. E. Steele, *J. Med. Chem*. **1991**, *34*, 725-736. c) D. Davey, P. W. Erhardt, W. C. Jr. Lumma, J. Wiggins, M. Sullivan, D. Pang, E. Cantor, *J. Med. Chem*.**1987**, *30*, 1337-1342. d) N. F. Ford, L. J. Browne, T. Campbell, C. Gemenden, R. Goldstein, C. Gude, J. W. F. Wasley, *J. Med. Chem*.**1985**, *28*, 164-170.

[20] Bioactivity of other substances with indolizine skeleton: a) D. Pla, A. Marchal, C. A. Olsen, A. Francesch, C. Cuevas, F. Albericio, M. Alvarez, *J. Med. Chem*. **2006**, *49*, 3257-3268. b) R. C. Oslund, N. Cermak, M. H. Gelb, *J. Med. Chem.* **2008**, *51*, 4708-4714. c) R. Liu, Y. Liu, Y.-D. Zhou, D. G. Nagle, *J. Nat. Prod.* **2007**, *70*, 1741-1745. d) F.Ishibashi, S. Tanabe, T. Oda, M. Iwao, *J. Nat. Prod.* **2002**, *65*, 500-504. e) M. Chittchang, P. Batsomboon, S. Ruchirawat, P. Ploypradith, *ChemMedChem* **2009**, *4*, 457-465. f) E. Marco, W. Laine, C. Tardy, A. Lansiaux, M. Iwao, F. Ishibashi, C. Bailly, F. Gago, *J. Med. Chem*. **2005**, *48*, 3796-3807. g) M. Facompre, C. Tardy, C. Bal-Mahieu, P. Colson, C.Perez, I. Manzanares, C. Cuevas, C. Bailly, *Cancer Res*. **2003**, *63*, 7392-7399.

[21] a) X.-Y. Hou, J.-J. Wang, X. Wang, D.-S. Li, J.-W. Wang, *Z. Kristallogr.* **2007**, *222*, 57-58. b) A. Sood, M. T. Räisänen, E. Aitola, A. Sibaouih, E. Colacio, M. Ahlgren, M. Nieger, T. Repo, M. Leskelä, *Polyhedron* **2013**, *56*, 221-229. c) R. Wortmann, U. Flörke, B. Sarkar, V. Umamaheshwari, G. Gescheidt, S. Herres-Pawlis, G. Henkel, *Eur. J. Inorg. Chem.* **2011**, *2011*, 121-130.

[22] a) T. Ito, T. Igarashi, H. Hagihara, *Acta Cryst. Section B* **1969**, *25*, 2303-2309. b) H. Spikes, *Tribology Letters* **2004**, *17*, 469-489.

[23] a) M. Shimoi, A. Ouchi, M. Aikawa, S. Sato, Y. Saito, *Bull. Chem. Soc. Jpn* **1982**, *55*, 2089-2093. b) M. G. B. Drew, M. Hasan, R. J. Hobson, D. A. Rice, *Dalton Trans.* **1986**, 1161-1166. c) P. G. Harrison, M. J. Begley, T. Kikabhai, F. Killer, *Dalton Trans.* **1986**, 929-938. d) L. Jeremias, G. Demo, V. Kubát, Z. Trávníček, J. Novosad, *Phosphorus, Sulfur, and Silicon and the Related Elements* **2014**, *189*, 1475-1488.

[24] K.A. Paseshnichenko, K. A. Aslanov, L.A. Yatsenko, A.V. Medvedev, S.V. *Koord. Khim.* **1984**, *10*, 1279.

[25] a) P. Ghosh, A. Roychowdhury, M. Corbella, A. Bhaumik, P. Mitra, S. M. Mobin, A. Mukherjee, S. Basu, P. Banerjee, *Dalton Trans.* **2014**, *43*, 13500-13508. b) S. M. Scott, K. C. Gordon, A. K. Burrell, *Dalton Trans.* **1998**, 2873-2878. c) L. M. Engelhardt, C. Pakawatchai, A. H. White, P. C. Healy, *Dalton Trans.* **1985**, 125-133. d) W. R. Tikkanen, C. Krueger, K. D. Bomben, W. L. Jolly, W. Kaska, P. C. Ford, *Inorg. Chem.* **1984**, *23*, 3633-3638.

[26] a) C. M. Alvarez, R. Garcia-Rodriguez, D. Miguel, *Dalton Trans.* **2007**, *692*, 3546-3554. b) C. M. Alvarez, R. Garcia-Rodriguez, D. Miguel, *J. Organomet. Chem.* **2007**, *692*, 5717-5726. c) C. M. Alvarez, R. Garcia-Rodriguez, J. M. Martin-Alvarez, D. Miguel, *Dalton Trans.* **2010**, *39*, 1201-1203. d) C. M. Alvarez, R. Garcia-Rodriguez, D. Miguel, *Inorg. Chem.* **2012**, *51*, 2984-2996.

[27] L. A Garcia-Escudero, D. Miguel, J. A. Turiel, *J. Organomet. Chem.* **2006**, *691*, 3434-3444.

[28] a) H. Ben Ammar, J. Le Nôtre, M. Salem, T. Mohamed, L. Kaddachi, J.-L. Toupet, C. Renaud, C. Bruneau and P. H. Dixneuf, *Eur. J. Inorg. Chem.* **2003**, *2003*, 4055-4064. b) H. Brunner, *Eur. J. Inorg. Chem,* **2001**, 905-912. (c) O. Dayan, S. Demirmen, N. Özdemir, *Polyhedron* **2015**, *85*, 926-932. d) I. de los Rios, M. J. Tenorio, J. Padilla, M. C. Puerta, P. Valerga, *Dalton Trans.* **1996**, 377-381. e) R. Lalrempuia, M. Rao Kollipara, *Polyhedron* **2003**, *22*, 3155-3160. f) P. Pelagatti, A. Bacchi, F. Calbiani, M. Carcelli, L. Elviri, C. Pelizzi, D. Rogolino, *J. Organomet. Chem.* **2005**, *690*, 4602-4610.

[29] a) D.E Coldbery, W.C. Fernelius, M. SHAMMA, *Inorg. Synth.* **1960**, *6*, 142. b) C.W. Watt, B. J. McCormick, *J. Inorg. Nucl. Chem.* **1965,** *27*, 898. c) Ö. Metin, L. T. Yıldırım and S. Özkar, *Inorg. Chem. Commun.* **2007**, *10*, 1121-1123.

[30] J. Díez, S. Falagán, P. Gamasa and J. Gimeno, *Polyhedron* **1988**, *7*, 37-42.

[31] E. W. Abel, G. Wilkinson, *J. Chem. Soc.* **1959**, 1501.

[32] E. W. Abel, G. Wilkinson, *J. Chem. Soc.* **1959**, 3149.

[33] M. A. Benet, T. N. Huang, T. W. Matheson, A. K. Smith, *Inorg. Synth.* **1982**, *21*, 74.

[34] Gaussian 09, Revision B.01, M. J. Frisch, G. W. Trucks, H. B. Schlegel, G. E. Scuseria, M. A. Robb, J. R. Cheeseman, G. Scalmani, V. Barone, B. Mennucci, G. A. Petersson, H. Nakatsuji, M. Caricato, X. Li, H. P. Hratchian, A. F. Izmaylov, J. Bloino, G. Zheng, J. L. Sonnenberg, M. Hada, M. Ehara, K. Toyota, R. Fukuda, J. Hasegawa, M. Ishida, T. Nakajima, Y. Honda, O. Kitao, H. Nakai, T. Vreven, J. A. Jr. Montgomery, J. E. Peralta, F. Ogliaro, M. Bearpark, J. J. Heyd, E. Brothers, K. N. Kudin, V. N. Staroverov, T. Keith, R. Kobayashi, J. Normand, K. Raghavachari, A. Rendell, J. C. Burant, S. S. Iyengar, J. Tomasi, M. Cossi, N. Rega, J. M. Millam, M. Klene, J. E. Knox, J. B. Cross, V. Bakken, C. Adamo, J. Jaramillo, R. Gomperts, R. E. Stratmann, O. Yazyev, A. J. Austin, R. Cammi, C. Pomelli, J. W. Ochterski, R. L. Martin, K. Morokuma, V. G. Zakrzewski, G. A. Voth, P. Salvador, J. J. Dannenberg, S. Dapprich, A. D. Daniels, O. Farkas, J. B. Foresman, J. V. Ortiz, J. Cioslowski, D. J. Fox, Gaussian, Inc., Wallingford CT, **2010**.

[35] A. D. Becke, *J. Chem. Phys.* **1993**, *98*, 5648-5652.
[36] C. Lee, W. Yang, R. G. Parr, *Phys. Rev. B* **1988**, *37*, 785-789.
[37] P. J. Hay, W. R. Wadt, *J. Chem. Phys.* **1985**, *82*, 299-310.
[38] a) P. C. Hariharan, J. A. Pople, *Theor. Chim. Acta* **1973**, *28*, 213-222. b) G. A. Petersson, M. A. Al-Laham, *J. Chem. Phys.* **1991**, *94*, 6081-6090. c) G. A. Petersson, A. Bennett, T. G. Tensfeldt, M. A. Al-Laham, S W. A.hirley, J. Mantzaris, *J. Chem. Phys.* **1988**, *89*, 2193-2218.
[39] CrysAlisPro-Data collection and integration software, version 1.171.37.35. Agilent Technologies UK Ltd, Oxford, UK, **2011**.
[40] G. M. Sheldrick, *Acta Cryst.* **2008,** *A64,* 112-122.
[41] O.V. Dolomanov, L.J. Bourhis, R.J. Gildea, J.A.K. Howard, H. Puschmann, OLEX2: *A complete structure solution, refinement and analysis program*. *J. Appl. Cryst.*, **2009**, *42*, 339-341.
[42] MERCURY: a) I. J. Bruno, J. C. Cole, P. R. Edgington, M. K. Kessler, C. F. Macrae, P. McCabe, J. Pearson, R. Taylor, *Acta Crystallogr*. **2002**, *B58*, 389-397. b) C. F. Macrae, P. R. Edgington, P. McCabe, E. Pidcock, G. P. Shields, R. Taylor, M.,Towler, J. van de Streek, *J. Appl. Crystallogr.* **2006**, *39*, 453-457.

Table 4. Crystal, measurement and refinement data for the compounds studied by X-ray diffraction.

	1	**2**	**3**	**4**
Formula	$C_{20}H_{29}N_3NiO_4P_2S_4$	$C_{18}H_{19}N_3NiO_2S_4$	$C_{23}H_{24}N_3NiO_{4.25}$	$C_{36}H_{27}F_{12}N_9NiP_2$
M_f	624.35	496.31	469.16	934.32
crystal system	monoclinic	triclinic	monoclinic	monoclinic
space group	$P2_1/n$	$P\bar{1}$	$P2/c$	$P2_1/c$
a [Å]	10.4523(7)	7.3985(6)	15.6368(6)	13.7831(6)
b [Å]	17.5400(10)	9.8601(9)	9.1700(3)	16.1496(5)
c [Å]	16.0259(9)	15.2496(10)	16.5248(5)	18.1157(8)
α [º]	90	84.298(6)	90	90.00
β [º]	106.868(6)	78.368(6)	102.696(3)	105.266(5)
γ [º]	90	70.367(8)	90	90.00
V [Å^3]	2811.7(3)	1025.66(15)	2311.55(14)	3890.1(3)
Z	4	2	4	4
ρ [Mgm^{-3}]	1.475	1.607	1.348	1.595
μ(Mo Kα) [mm^{-1}]	1.132	1.373	0.873	0.680
crystal size [mm]	0.2572 × 0.1868 × 0.1011	0.1747 × 0.1637 × 0.0889	0.2264 × 0.1334 × 0.0866	0.2085 × 0.0977 × 0.0718
F(000)	1296.0	512.0	980.0	1888.0
θ range [º]	4.166 to 57.23	4.388 to 57.16	4.442 to 57.45	4.18 to 59.64
Max./min. transmission	0.911/0.848	0.903/0.833	0.940/0.878	0.957/0.909
reflns collected	12076	6836	9805	22177
indep. refl. [R(int)]	6372 [0.0528]	4596 [0.0227]	5245 [0.0339]	9462 [0.1023]
GOF on F^2	1.044	1.040	1.060	0.943
parameters/restraints	0/311	0/255	4/298	0/541
R_1 (on F, $I > 2\square(I)$)	0.0669	0.0442	0.0635	0.0887
wR_2(on F^2, all data)	0.2161	0.0942	0.2101	0.2867
Max/min $\Delta\rho$ [eÅ^{-3}]	0.53/-0.34	0.41/-0.35	0.97/-0.32	1.50/-0.43
CCDC number	1400079	1400080	1400081	1400082

	6	7	8	9
Formula	$C_{24}H_{18}Cl_4Mn_2N_6$	$C_{24}H_{18}Cl_2MnN_6$	$C_{20}H_{29}N_3O_4P_2S_4Zn$	$C_{20}H_{29}CdN_3O_4P_2S_4$
M_f	642.12	516.28	631.01	678.04
crystal system	triclinic	orthorhombic	monoclinic	monoclinic
space group	$P\bar{1}$	*Pbca*	$P2_1/n$	$P2_1/c$
a [Å]	8.7623(7)	15.4323(4)	9.1545(2)	10.5417(2)
b [Å]	9.3685(7)	13.8100(4)	21.1326(5)	17.4921(3)
c [Å]	9.4971(9)	20.7561(5)	15.1624(3)	16.6087(3)
α [°]	64.965(8)	90.00	90	90
β [°]	62.893(9)	90.00	95.980(2)	108.0565(18)
γ [°]	84.890(6)	90.00	90	90
V [Å^3]	623.54(9)	4423.5(2)	2917.34(11)	2911.73(9)
Z	1	8	4	4
ρ [Mgm^{-3}]	1.710	1.550	1.437	1.547
μ(Mo Kα) [mm^{-1}]	1.469	0.865	1.268	1.177
crystal size [mm]	0.1891 × 0.1166 × 0.0619	0.3474 × 0.1341 × 0.0826	0.6006 × 0.1425 × 0.0969	0.5411 × 0.2863 × 0.2088
F(000)	322.0	2104.0	1304.0	1376.0
θ range [°]	4.84 to 59.24	4.42 to 59.18	4.708 to 59.198	4.064 to 59.674
Max./min. transmission	0.963/0.922	1.000/0.876	0.921/0.565	0.799/0.651
reflns collected	4768	15606	15148	28176
indep. refl. [R(int)]	2901 [0.0246]	5421 [0.0378]	6877 [0.0300]	7367 [0.0253]
GOF on F^2	1.046	1.120	1.042	1.015
parameters/restraints	0/163	0/298	0/311	0/311
R_1 (on F, $I > 2\sigma(I)$)	0.0415	0.0467	0.0526	0.0475
wR_2(on F^2, all data)	0.0838	0.0815	0.1163	0.1351
Max/min $\Delta\rho$ [eÅ^{-3}]	0.37/-0.28	0.30/-0.42	0.40/-0.34	0.64/-0.45
CCDC number	1800084	1800083	1800085	1800086

	10	**11**	**12**	**13**
Formula	$C_{12}H_9I_4N_3Sn$	$C_{18}H_{14}Cl_3N_3Sn$	$C_{20}H_{27}Cl_2N_3Sn$	$C_{48}H_{39}BCuF_4N_3P_2$
M_f	821.51	497.36	499.03	870.11
crystal system	triclinic	monoclinic	monoclinic	triclinic
space group	$P\bar{1}$	$P2_1/n$	$P2_1/n$	$P\bar{1}$
a [Å]	7.2624(6)	11.0147(3)	9.7507(3)	10.0570(4)
b [Å]	10.3169(9)	15.9615(4)	12.3131(6)	14.5866(6)
c [Å]	12.9622(10)	12.0785(3)	18.2608(7)	14.8867(7)
α [°]	82.026(7)	90	90	81.173(4)
β [°]	76.078(7)	102.904(3)	95.247(3)	75.230(4)
γ [°]	74.172(8)	90	90	85.940(3)
V [Å^3]	904.15(14)	2069.92(10)	2183.24(15)	2085.52(17)
Z	2	4	4	2
ρ [Mgm^{-3}]	3.018	1.596	1.518	1.386
μ(Mo Kα) [mm^{-1}]	8.236	1.627	1.424	0.657
crystal size [mm]	0.3047 × 0.1546 × 0.0521	0.3387 × 0.1005 × 0.0696	0.27 × 0.1364 × 0.0748	0.5147 × 0.2394 × 0.2066
F(000)	728.0	976.0	1008.0	896.0
θ range [°]	4.116 to 57.222	4.298 to 57.374	3.994 to 57.454	4.19 to 57.48
Max./min. transmission	0.663/0.160	0.913/0.726	0.926/0.817	0.893/0.771
reflns collected	5710	8751	9855	13972
indep. refl. [R(int)]	4037 [0.0311]	4717 [0.0270]	4967 [0.0499]	9320 [0.0198]
GOF on F^2	1.156	1.093	1.066	1.027
parameters/restraints	0/181	0/226	0/237	0/532
R_1 (on F, $I > 2\sigma(I)$)	0.0544	0.0545	0.0551	0.0477
wR_2(on F^2, all data)	0.1443	0.2117	0.0977	0.1273
Max/min $\Delta\rho$ [eÅ^{-3}]	1.62/-1.20	2.55/-0.48	0.77/-0.50	0.67/-0.33
CCDC number	1800088	1800089	1800090	1800087

	14	**15**	**16**	**17**
Formula	$C_{15}H_9BrMnN_3O_3$	$C_{15}H_9BrN_3O_3Re$	$C_{16}H_9MoN_3O_4$	$C_{26}H_{31}ClF_6N_3OPRu$
M_f	414.10	545.36	403.20	683.03
crystal system	triclinic	triclinic	monoclinic	monoclinic
space group	$P\bar{1}$	$P\bar{1}$	$P2_1/n$	$C2/c$
a [Å]	7.2998(5)	7.1362(8)	6.1771(2)	31.8475(13)
b [Å]	10.6028(8)	10.7360(12)	18.8221(7)	9.9701(4)
c [Å]	10.6341(8)	10.8773(10)	13.6711(4)	18.0493(7)
α [º]	89.137(6)	100.086(9)	90	90.00
β [º]	86.392(6)	94.758(8)	100.944(3)	94.099(4)
γ [º]	73.945(6)	103.908(9)	90	90.00
V [Å^3]	789.38(10)	789.59(15)	1560.57(9)	5716.4(4)
Z	2	2	4	8
ρ [Mgm^{-3}]	1.742	2.294	1.716	1.587
μ [mm^{-1}]	(Cu Kα)9.928	(Mo Kα) 10.242	(Mo Kα) 0.866	(Mo Kα) 0.762
crystal size [mm]	0.2143 × 0.1221 × 0.0772	0.3418 × 0.0826 × 0.0785	0.2762 × 0.1315 × 0.0464	0.5203 × 0.2378 × 0.0491
F(000)	408.0	508.0	800.0	2768.0
θ range [º]	8.34 to 149.74	4.946 to 58.976	4.328 to 57.356	4.28 to 57.12
Max./min. transmission	0.587/0.333	0.520/0.120	0.961/0.887	0.964/0.766
reflns collected	5116	6182	6190	11879
indep. refl. [R(int)]	3121 [0.0231]	3655 [0.0320]	3498 [0.0269]	6459 [0.0331]
GOF on F^2	1.067	1.041	1.016	1.019
parameters/restraints	3121/0/209	3655/0/209	3498/0/217	6459/0/355
R_1 (on F, $I > 2\sigma(I)$)	0.0317	0.0372	0.0411	0.0575
wR_2(on F^2, all data)	0.0759	0.0587	0.0799	0.1586
Max/min $\Delta\rho$ [eÅ^{-3}]	0.23/-0.26	1.29/-1.00	0.50/-0.49	0.68/-0.43
CCDC number	1800091	1800092	1800093	1800094

Keywords: Chelate complexes / N ligands / Ligand effects / Ligand design / D-block metals

Entry for the Table of Contents

FULL PAPER

A thorough screening confirms the potential of the now easily available 3-(pyridin-2-yl)imidazo[1,5-a]pyridine (Py-indz) ligand in the preparation of complexes with transition and main-group metallic centers in very different environments.

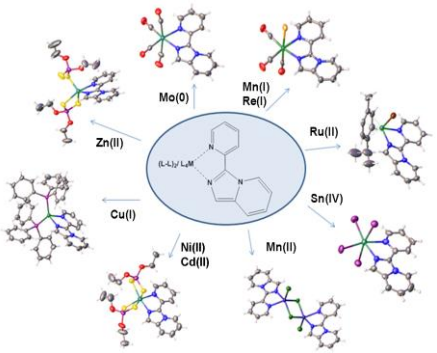

Alvarez, Celedonio; Alvarez-Miguel, Lucia; García-Rodríguez, Raúl; Martin-Alvarez, Jose; Miguel, Daniel.*

Universidad de Valladolid, IU CINQUIMA/Quimica Inorganica

Page No. – Page No.

Title

3-(pyridin-2-yl)imidazo[1,5-a]pyridine (pyridylindolizine) as ligands in complexes of transition and main-group metals.

*one or two words that highlight the emphasis of the paper or the field of the study